

# Design of a CMOS phase to digital transducer for optical incremental sensors<sup>☆</sup>

Cheng-Ta Chiang<sup>a,\*</sup>, Kaun-Chun Hsieh<sup>b</sup>, Yu-Chung Huang<sup>b</sup>

<sup>a</sup> Department of Electrical Engineering, National Chia-Yi University, Taiwan

<sup>b</sup> Measurement Techniques Laboratory, National Chiao Tung University, Hsin Chu, Taiwan

## ARTICLE INFO

### Article history:

Received 31 December 2010

Received in revised form 24 May 2011

Accepted 24 May 2011

Available online 31 May 2011

### Keywords:

Optical incremental sensors

Interpolation circuits

ADC

PLL

## ABSTRACT

In this paper, a CMOS phase to digital transducer for optical incremental sensors is newly proposed. The proposed chip can easily produce phase shifts of signals by using a resistor chain. A set of calibration circuits for optical incremental sensors is also designed in the proposed chip. Another innovation is that the outputs of the proposed chip are directly digitized; they could be easily sent over a wide range of transmission media, such as PSN, radio, optical, IR, ultrasonic, etc. Besides, it does not also need a ROM component or a fast counter as used in the structures of ADC-based and PLL-based interpolations. Based upon the device parameters of 0.5  $\mu\text{m}$  2P2M CMOS technology with 5 V power supply, all the functions and performance of the proposed CMOS phase to digital transducer for optical incremental sensors are successfully tested and proven through measurements. The area of the proposed chip including ESD I/O pads is  $2010 \times 1502 \mu\text{m}^2$ . The interpolation factor is 5, 10, and 40. The proposed chip is suitable for optical incremental sensors.

© 2011 Elsevier B.V. All rights reserved.

## 1. Introduction

The developments of precise measurement and positioning devices [1,2] have been used on the process, testing equipment of electronic and semiconductor industry. Smaller line width and more precise needs are required into nano-meter scale. Thus, the techniques of improving the accuracy and resolution on precise measurements are strongly required.

Except for the laser interferometer, the main positioning and displacement devices are linear encoders, which have the characteristics of lower cost. Among linear encoders, optical encoders are popular in modern electronic and semiconductor industry due to its characteristic of high-accuracy. Optical encoders, which consist of optical sensors and circuits, employ the light passing through the grating. Thus, the encoders generate periodic quadrature signals. The phases of these quadrature signals are relative to the movement of the grating. However, the accuracy is still restricted by optical properties and mechanical assembly. In order to improve the accuracy and resolution of optical encoders, a technique of interpolation is developed [3–10]. It improves the resolution of optical encoders by doing the subdivision of the phases. Previous method [3,4] utilizes a phase-locked loop (PLL) to achieve the

interpolation. However, these achievements should design an oscillator to synthesize frequency. The design of a high-frequency PLL, which is with precision locked frequency and good linearity of an oscillator, is rather difficult. Another method [5–8], which uses an analog-to-digital converter (ADC), is used to perform the interpolation. However, this scheme needs a ROM component to perform the function of look-up table. The technology and ROM size will be another considerable issue. Besides, this scheme may need a higher system clock. For example, previous work [6] requires a clock frequency of 30 MHz. Hence, a technique, which is based on comparator-based interpolation [9,10], is proposed. However, Stephens et al. [9] and Rieder et al. [10] need to use 4 and 3 sine signals to generate signals with different phases. The processing circuits are complicated. Another issue of the interpolation error should also be discussed. The phase delay and frequency jitter of PLL produce the interpolation error of PLL-based interpolation. This error is basically related to the circuit structure of PLL. The interpolation error of ADC-based interpolation is caused by the resolution, response time, and accuracy of ADC. Although the interpolation error can be reduced by using a high resolution ADC, the response time also increases. Besides, the accuracy is related to the circuit structure of ADC. For example, nonlinear effect of ADC is a problem on the ADC-based interpolation. The interpolation error of comparator-based interpolation comes from the finite DC gain and response time of comparator. The interpolation error can be reduced by increasing the finite DC gain and speeding up the transient response of a comparator. Compared with ADC-based and PLL-based interpolations, the interpolation error of comparator-based interpolation is easily reduced by designing on the circuit

<sup>☆</sup> This work was supported by the National Science Council, Taiwan, under contracts NSC-99-218-E-415-002.

\* Corresponding author. Tel.: +886 5 2717587; fax: +886 5 2717558.

E-mail addresses: [ctchiang@mail.ncyu.edu.tw](mailto:ctchiang@mail.ncyu.edu.tw), [ctchiang23@yahoo.com.tw](mailto:ctchiang23@yahoo.com.tw) (C.-T. Chiang).

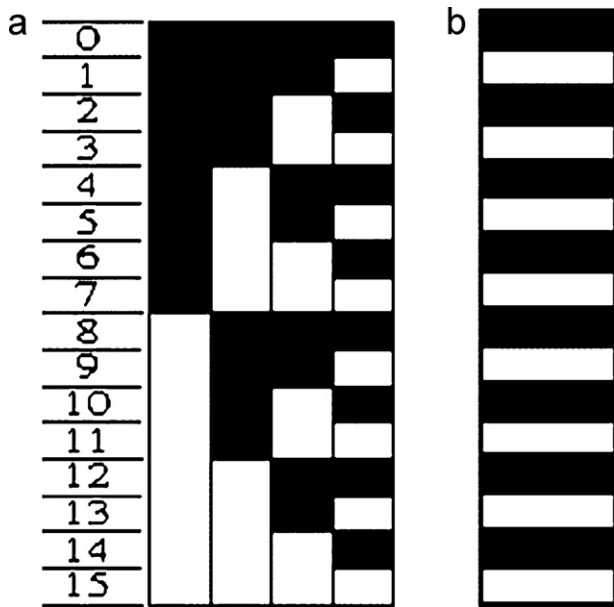


Fig. 1. (a) Optical absolute sensors and (b) optical incremental sensors.

structure of a uniform comparator. Different to previous works, an improved method [11] of comparator-based interpolation is proposed. The proposed chip can easily produce phase shifts of signals by using a resistor chain. A set of calibration circuits for optical incremental sensors is also designed in the proposed chip. Another innovation is that the outputs of the proposed chip are directly digitized; they could be easily sent over a wide range of transmission media, such as PSN, radio, optical, IR, ultrasonic, etc. Besides, it does not also need a ROM component or a fast counter as used in the structures of ADC-based and PLL-based interpolations. Relative to this work, a digital-to-phase converter is discussed in [12,13]. However, they are mainly researched on high-speed PLL or delay-locked loop (DLL). In this work, we propose an improved method and openly demonstrate how to implement a phase to digital transducer for optical incremental sensors. Readers can understand whole design techniques from this work, and this is the main contribution of this work.

In this paper, a CMOS phase to digital transducer for optical incremental sensors is newly proposed and designed in CMOS 0.5  $\mu\text{m}$  2P2M process with 5 V power supply. The area of the proposed chip including ESD I/O pads is  $2010 \times 1502 \mu\text{m}^2$ . The power consumption is 50 mW. The proposed chip is suitable for optical incremental sensors.

In Section 2, the overview of optical incremental sensors is addressed. Section 3 discusses system architecture and simulation results. Section 4 demonstrates the measurements. Finally, conclusions and future works are described.

## 2. The overview of optical incremental sensors

Optical sensors used in the optical encoders can be distinguished into two types as shown in Fig. 1. One is optical absolute sensors and the other is optical incremental sensors. The difference between them is in the arrangements of optical grating. The distance of optical grating of incremental type is designed in equal space. The output signals are periodic signals. However, the arrangements of absolute type are totally different. The output signals just correspond to its absolute position. The design of optical grating of incremental type is easier than that of absolute type. In this paper, the incremental type is chosen and its corresponding circuit is proposed. However, due to congenital features of incremental type,

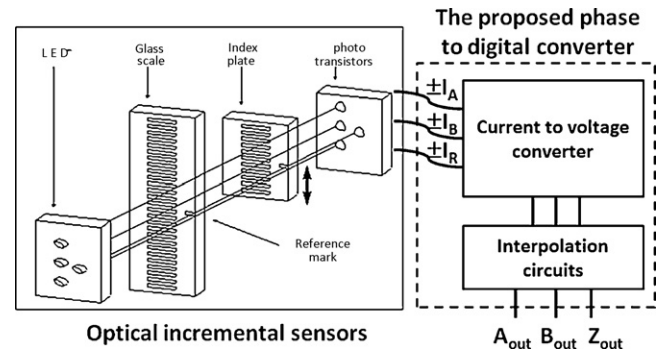


Fig. 2. Optical incremental sensors and the proposed phase to digital transducer.

measurement errors will be always accumulated. Thus, optical incremental sensors need to perform the extra calibration to eliminate the accumulated errors. The calibration method is to add a design of reference mask. As shown in Fig. 2, when a glass scale and an index plate have a relative movement, the lighting intensity of photo transistors will be changed. The output signals can be viewed as waves which are similar to sine signals as shown in Fig. 3. The output currents of optical incremental sensors are  $I_A$ ,  $I_B$ , and  $I_R$ .  $I_A$  and  $I_B$  are the main input sources of the proposed chip.  $I_R$  is the current used to calibrate the accumulated errors. The period of  $I_A$  and  $I_B$  is equal to the width of an optical grating. To calculate the numbers of the period is to obtain the distance of the movement.

The resolution of optical increment sensors is limited by the width of an optical grating. If the resolution needs to increase, the width of an optical grating must also be shortened. However, the technique to make the width be less than 1  $\mu\text{m}$  is rather difficult. Besides, the effects of diffraction and noise will be serious problems. This work proposes an improved method to do the subdivision of the phases. By using the proposed method, resolution can be increased without changing the width of an optical grating. The specification of the optical incremental sensor can be captured from [14]. In Section 4, the optical incremental sensor will be applied and experimented on the proposed phase to digital transducer. In the following sections, all the discussions of system architecture, simulation, and measurement results will be discussed.

## 3. System architecture and simulation results

The proposed CMOS phase to digital transducer for optical incremental sensors includes a current to voltage converter and interpolation circuits. The interpolation circuits as shown in Fig. 4 implement a resistor chain, comparators, and the digital processing circuits. The signals of  $V_A$ ,  $V_{A-}$ ,  $Z_{in}$ , and  $V_B$  are connected to the outputs of the current to voltage converter. The signals of  $A_{out}$ ,  $B_{out}$ , are the digitized outputs. The output signal of  $Z_{out}$  is used to calibrate the accumulated errors of optical incremental sensors. The signal of  $A_{com}$  is the common-mode voltage. The current of  $I_{ref}$  is the bias current of comparators. The signals of  $SeI_0$  and  $SeI_1$  can decide the interpolation factor of 5 or 10. The signal of  $En$  is an enable signal, which can turn on or off the chip.

Fig. 5 shows the basic principle of the proposed phase-shift method. A resistor chain is built to implement the phase-shift method. The pulse signal of  $V_D$  is the output of a comparator and the signal of  $V_S$  is a phase-shift signal with phase  $\phi$ . The phase difference of  $V_A$  and  $V_B$  is  $90^\circ$ . According to the superposition theorem, the voltage of  $V_S$  can be obtained as

$$V_S = \frac{R_2}{R_1 + R_2} \sin(\theta) + \frac{R_1}{R_1 + R_2} \cos(\theta) = \frac{\sqrt{R_1^2 + R_2^2}}{R_1 + R_2} \times \sin(\theta + \phi) \quad (1)$$

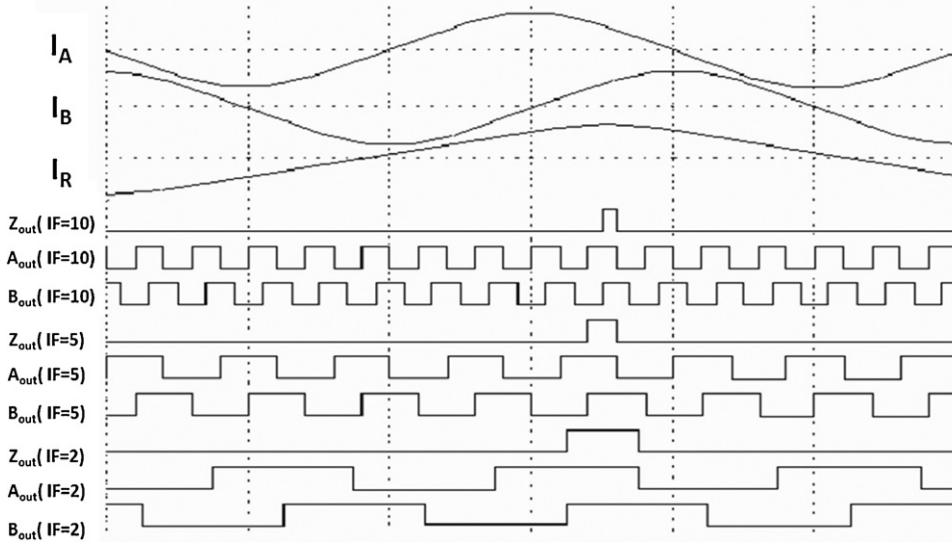


Fig. 3.  $I_A$ ,  $I_B$ , and  $I_R$  are the output currents of optical incremental sensors.  $A_{out}$ ,  $B_{out}$ ,  $Z_{out}$  are the outputs of the proposed phase to digital transducer. The number of  $IF$  is the interpolation factor.

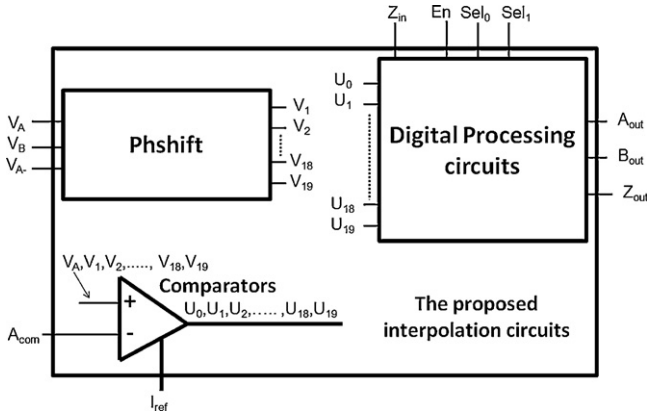


Fig. 4. The circuit diagram of the proposed interpolation circuits.

and

$$\cot \phi = \frac{R_2}{R_1} \quad (2)$$

where  $\phi$  is the shift phase. By (2), when the ratio of  $R_1$  and  $R_2$  is chosen, the  $\phi$  is attained. In Fig. 6, the signal of  $V_\phi$  is acquired by using a XOR logic gate. That means that the  $V_\phi$  is generated from the XOR logic function of  $V_{DS}$  and  $V_{DA}$ . The function of interpolation is implied in the signal of  $V_\phi$ . Similarly, the proposed method can be extended into the interpolation factor of  $N$  as shown in Fig. 7. The phase difference of  $\Delta\phi$  within each resistor is a fixed phase of  $\phi$ . By following (1) and (2), each resistor  $R_M$  within a resistor chain

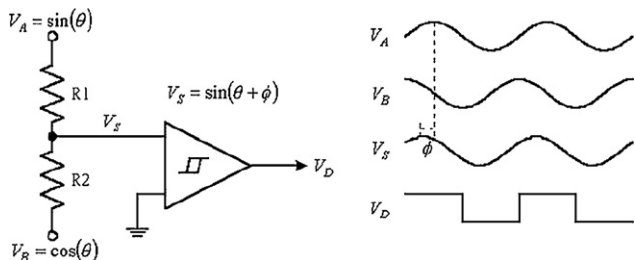


Fig. 5. The basic principle of the proposed phase-shift method.

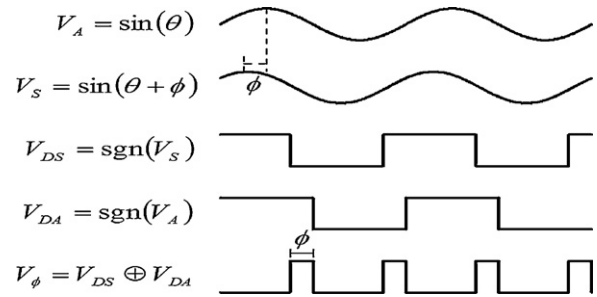


Fig. 6. The waveform of  $V_\phi$ .

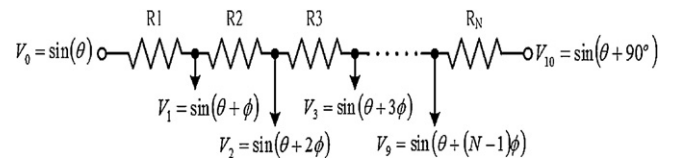


Fig. 7. The divisions of phases with the interpolation factor  $N$ . In this example,  $N$  is 10.

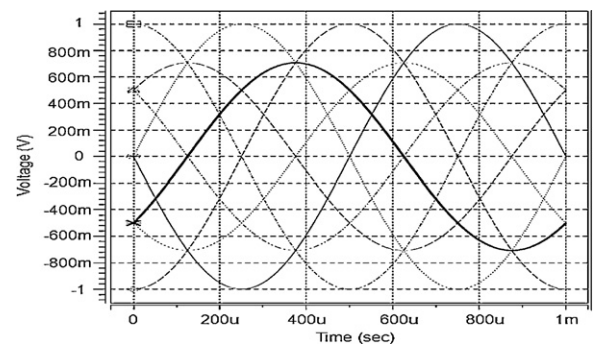


Fig. 8. SPICE simulations of the proposed phase-shift method. The interpolation factor is 8.

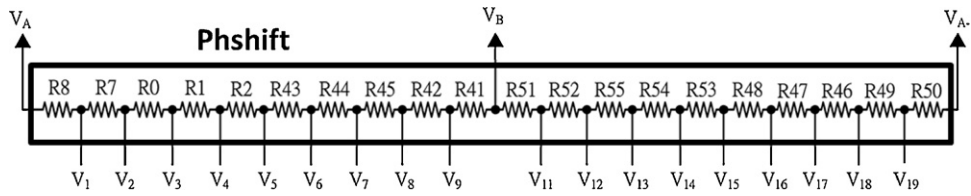


Fig. 9. The circuit diagram of phase shift shown in Fig. 4.

is derived as

$$R_M = R_{total} \times \left[ \frac{1}{1 + \cot[(M/N) \times 90^\circ]} - \sum_{i=1}^{M-1} \frac{1}{1 + \cot[(i/N) \times 90^\circ]} \right] \quad (3)$$

where  $M$  represents the assigned number of each resistor, and  $R_{total}$  is the total resistance of a resistor chain. By (1)–(3), the phases can be easily divided by a resistor chain. For example, if  $N$  is 10 and  $R_{total}$  is 1 M $\Omega$ , 10 resistors of  $R_1$  to  $R_{10}$  are 137 k $\Omega$ , 109 k $\Omega$ , 92 k $\Omega$ , 83 k $\Omega$ , 79 k $\Omega$ , 83 k $\Omega$ , 83 k $\Omega$ , 92 k $\Omega$ , 109 k $\Omega$ , and 137 k $\Omega$ , respectively. As shown in Fig. 8, eight phases within a resistor chain are successfully shifted.

In circuit implementation, Fig. 9 shows the circuit diagram of phase shift shown in Fig. 4. The signals of  $V_1$  to  $V_{19}$  with different phases are generated and connected to the inputs of comparators. Fig. 10 demonstrates the circuit diagram of digital processing circuits shown in Fig. 4. The signals of  $U_0$  to  $U_{19}$  are the output signals of comparators. They are used to perform digital processing procedures through the circuits of interpolation A and B, and the circuit of zais A and B. The circuit diagram of interpolation A and B is displayed in Fig. 11. The output signals of  $A_{out}$ ,  $B_{out}$  can be attained by performing XOR logic gate. The circuit diagram of zais A and B is built by a 3-input AND logic gate. In the design of comparators, noise is always a considerable problem. In order to decrease erroneous judgements, comparators need to have a hysteresis voltage. The circuit is displayed in Fig. 12, and the hysteresis is derived as

$$V_{SPH} = Vin_+ - Vin_- = \frac{Iss}{gm} \times \frac{(\beta_B/\beta_A) - 1}{(\beta_B/\beta_A) + 1} \quad \text{for } \beta_B \geq \beta_A \quad (4)$$

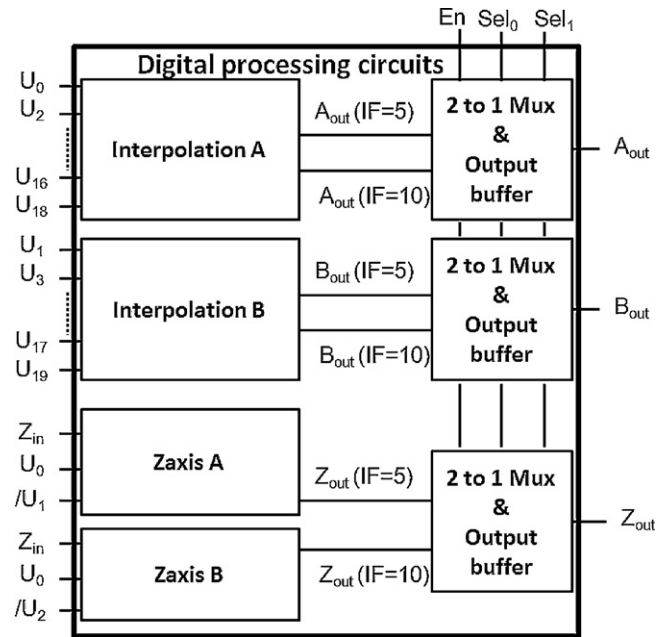


Fig. 10. The circuit diagram of digital processing circuits shown in Fig. 4.

and

$$V_{SPL} = -V_{SPH}, \beta_B = \beta_6 = \beta_7, \beta_A = \beta_5 = \beta_8 \quad (5)$$

where  $gm$  is the transconductance of the MOSFET, the parameter of  $\beta$  is defined as  $\mu_n C_{ox} W/L$ , and  $V_{SPL}$  and  $V_{SPH}$  are half of hystere-

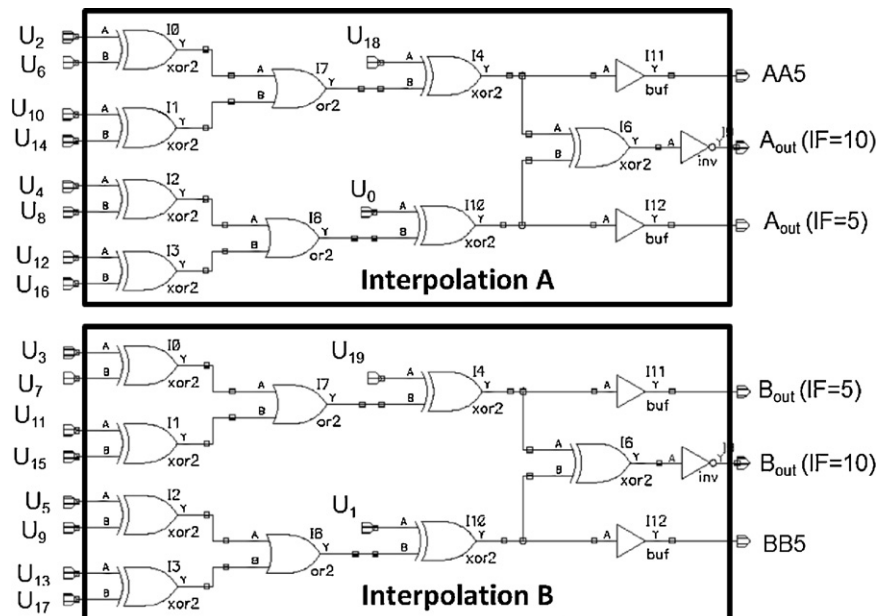


Fig. 11. The circuit diagram of interpolation A and B shown in Fig. 10.

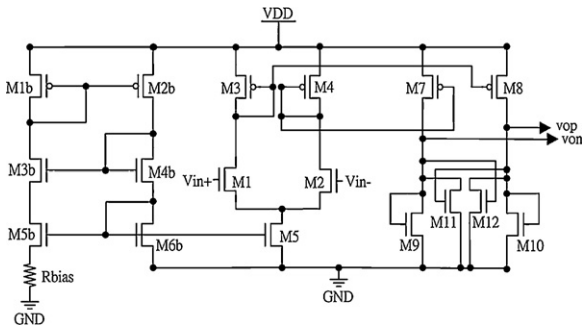


Fig. 12. Circuit schematic of the comparator.

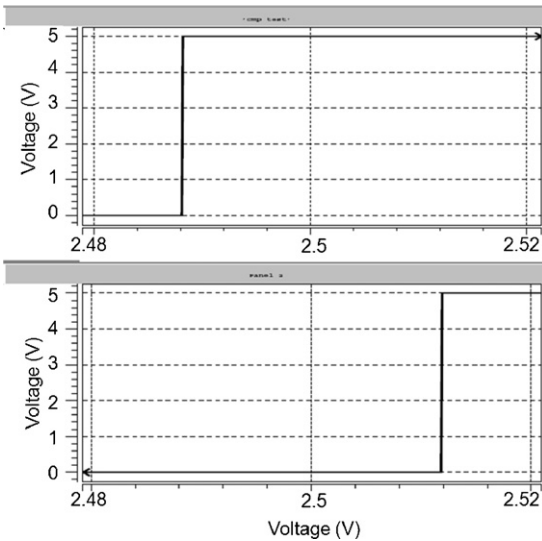


Fig. 13. SPICE simulations of the hysteresis of the comparator.

Table 1  
The specification of the comparators.

$V_{offset}$	10 mV
$V_{hysteresis}$	24 mV
DC gain	5000
Delay time	50 ns
VDD	5 V
$I_{DD}$	0.5 mA

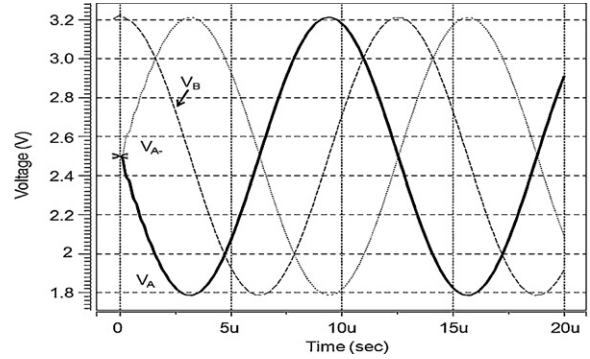


Fig. 15. SPICE simulations of the current to voltage converter.

sis voltage. After simulations, the hysteresis is 24 mV as shown in Fig. 13. The design specifications of comparators are listed in Table 1. Fig. 14 demonstrates the circuit schematic of the current to voltage converter connected to optical incremental sensors. The currents generated by sensors are  $I_{\pm A}$ ,  $I_{\pm B}$ , and  $I_{\pm R}$ . Converted by the current to voltage converter, each corresponding voltages of  $V_A$ ,  $V_{A-}$ , and  $V_B$ , are obtained as shown in Fig. 15.

Finally, the whole circuits are built and simulated. The output signals of  $A_{out}$ ,  $B_{out}$ , and  $Z_{out}$  under the interpolation factor of 10 and 5 are demonstrated in Figs. 16 and 17, respectively. As demonstrated, these outputs are successfully attained. The test of integral nonlinearity (INL) and differential nonlinearity (DNL) are verified in

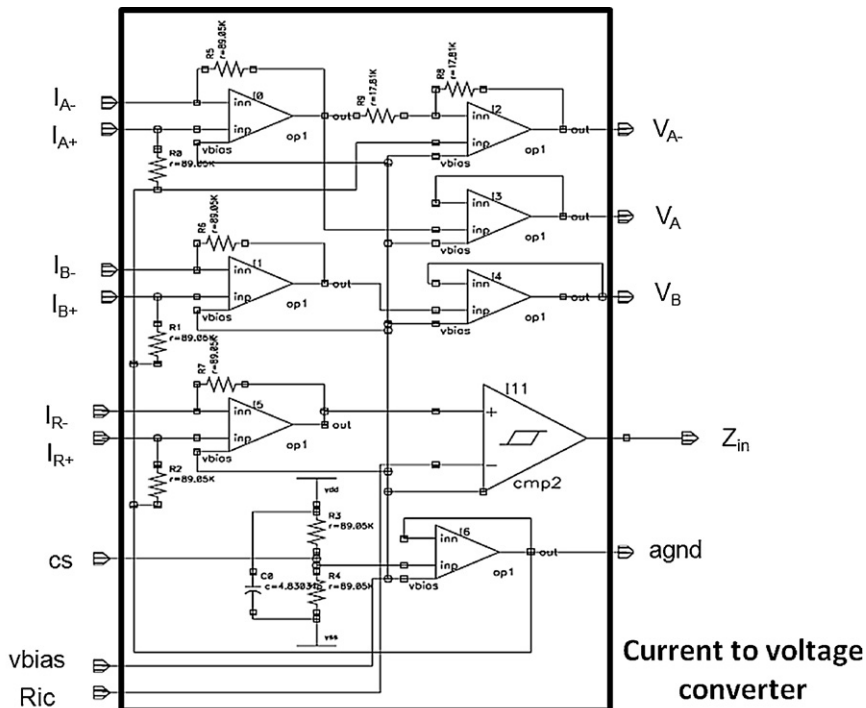


Fig. 14. Circuit schematic of the current to voltage converter connected to optical incremental sensors.

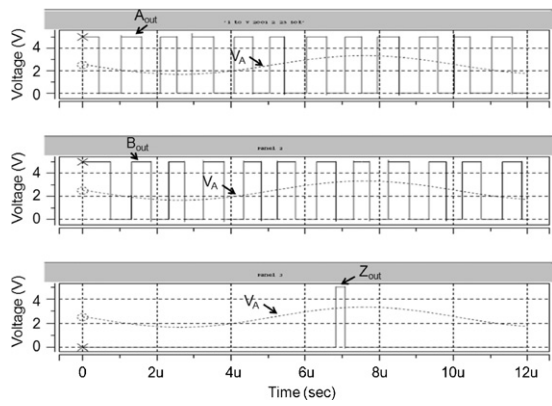


Fig. 16. SPICE simulations of  $A_{out}$ ,  $B_{out}$ , and  $Z_{out}$  under the interpolation factor of 10.

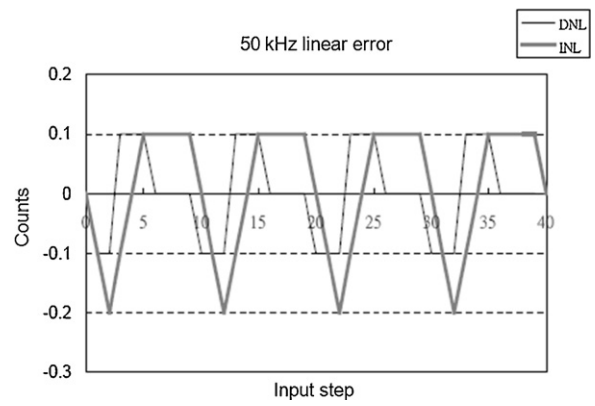


Fig. 18. The INL and DNL.

Fig. 18. Both of them are all less than 1 count, and indicate that the proposed chip has a good linearity. Although the interpolation factor can just be chosen 5 or 10, the outputs under the interpolation factor of 40 can be easily obtained by performing the XOR logic function of  $A_{out}$  ( $IF=10$ ) and  $B_{out}$  ( $IF=10$ ). However, it is optional for user choice. All the functions and performance of the proposed phase to digital transducer for optical incremental sensors are successfully tested and proven through SPICE simulations.

4. Measurement results

Fig. 19 demonstrates the microphotograph of the proposed CMOS phase to digital transducer for optical incremental sensors. In this work, the CMOS 0.5  $\mu\text{m}$  2P2M process with 5 V power supply is chosen due to its lower cost to fabricate this chip. The chip area including ESD I/O pads is  $2010 \times 1502 \mu\text{m}^2$ . The power consumption is 50 mW. The measurement setup is built as shown in Fig. 20. A logic analyzer is to generate digital codes from two sine signals that have the phase difference of  $90^\circ$ . Undoubtedly, these two codes also have the phase difference of  $90^\circ$ . The currents of  $\pm I_A$  and  $\pm I_B$  are obtained from a digital to analog converter (DAC) and voltage to current converters marked as v2i. The current of  $\pm I_R$  can be easily generated by a signal generator. Fig. 21 demonstrates

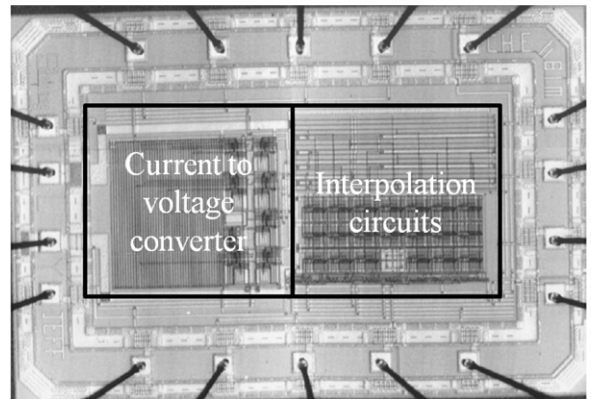


Fig. 19. The microphotograph of the proposed CMOS phase to digital transducer for optical incremental sensors is  $2010 \times 1502 \mu\text{m}^2$  including ESD I/O pads.

the measurement results under the interpolation factor of 5 and 10, respectively. The signal frequency is 50 kHz. As shown, the output signals are successfully proven. The test of the INL and DNL is displayed in Fig. 22. The INL is less than 0.8 count and DNL is less than 0.5 count. Although the value is slightly increased, it is still

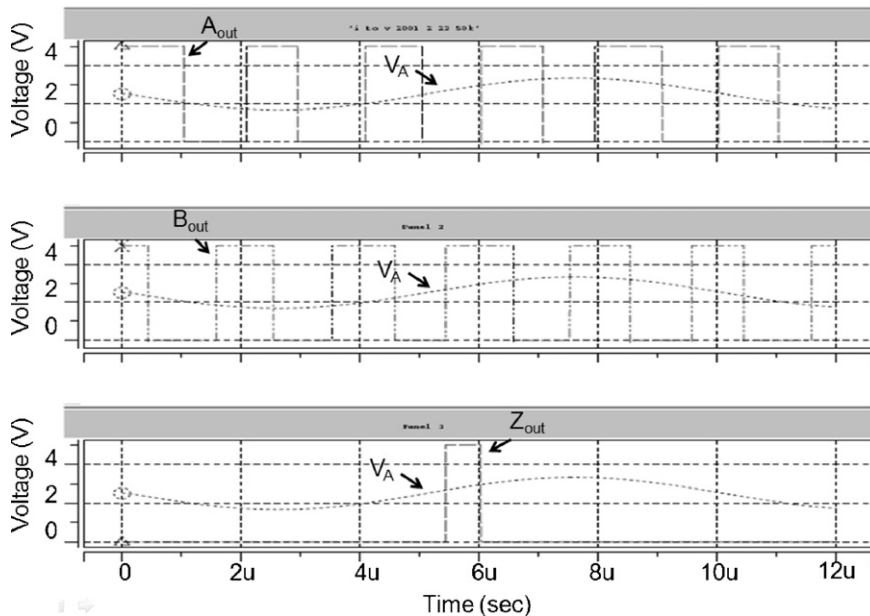


Fig. 17. SPICE simulations of  $A_{out}$ ,  $B_{out}$ , and  $Z_{out}$  under the interpolation factor of 5.

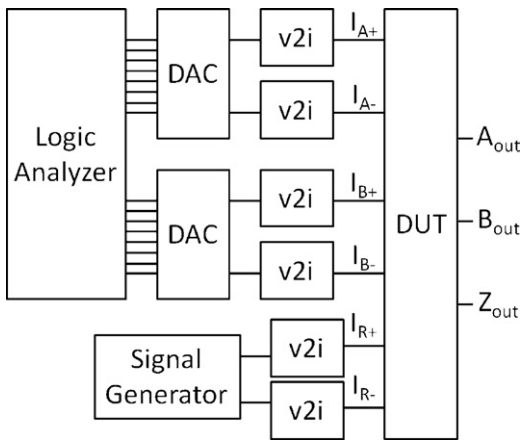


Fig. 20. The measurement setup.

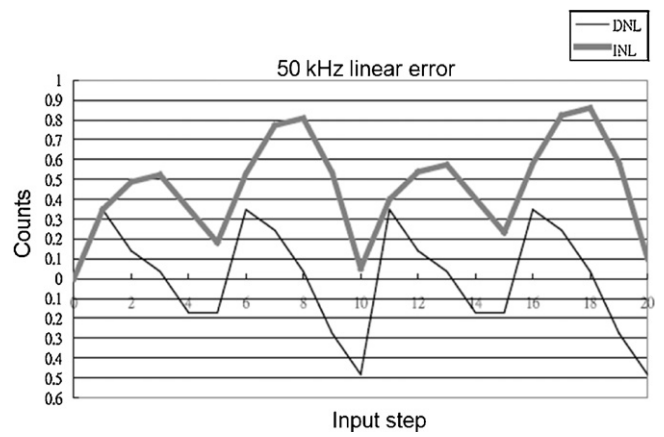


Fig. 22. The INL and DNL of the measurement results under the interpolation factor of 10. The signal frequency is 50 kHz.

**Table 2**  
Summary on the characteristics of the proposed CMOS phase to digital transducer for optical incremental sensors.

Technology	0.5 $\mu\text{m}$ CMOS 2P2M
Power supply	5 V
Interpolation factor	5, 10, 40 (optional)
Signal amplitude	$\pm 0.2$ to $\pm 0.8$ V
Signal bandwidth	50 kHz
Sampling frequency	Do not need
Power consumption	50 mW
Physical layout of the proposed chip	2010 $\times$ 1502 $\mu\text{m}^2$
Application field	Optical incremental sensors

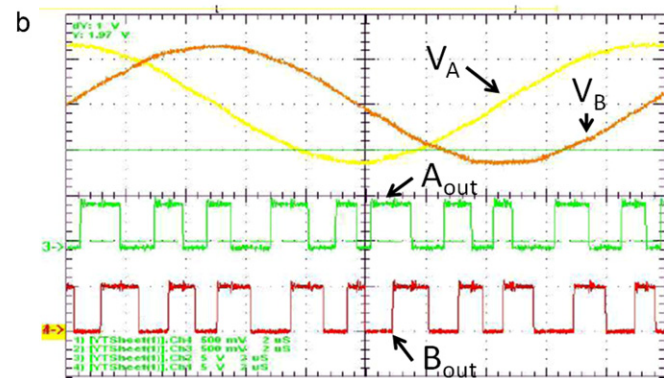
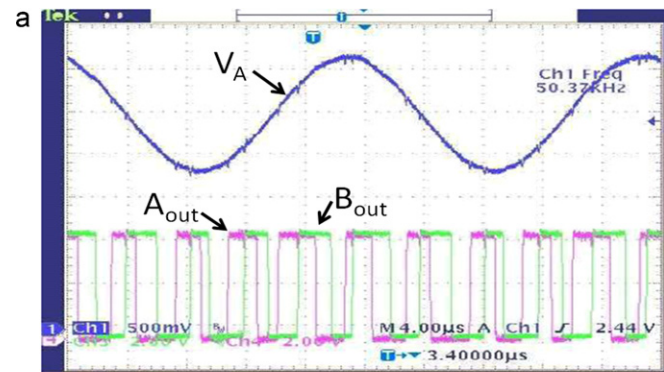
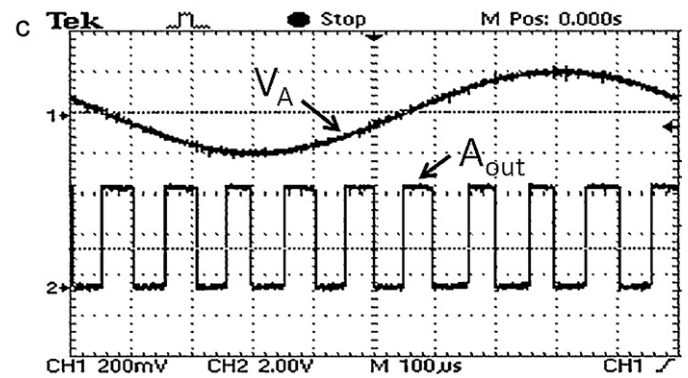
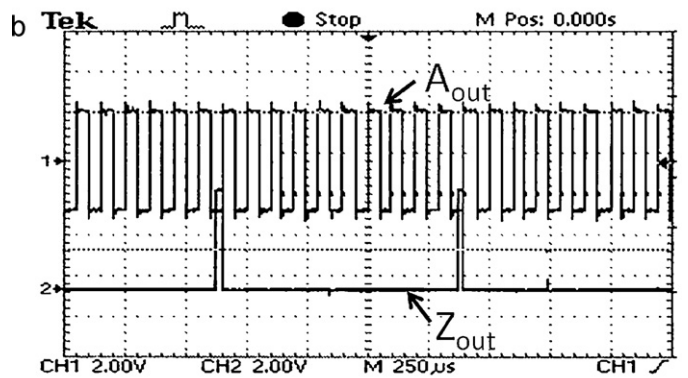
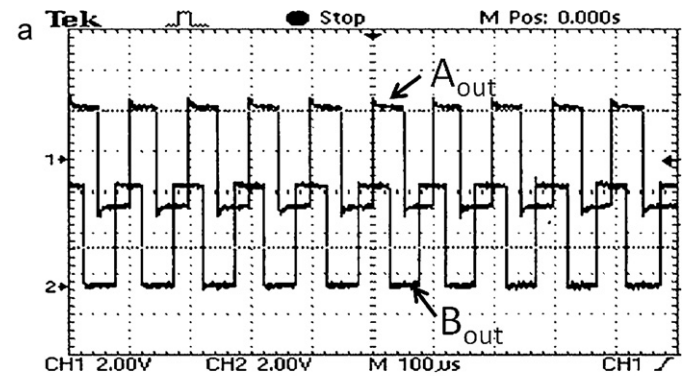


Fig. 21. The measurement results under the interpolation factor of (a) 5 and (b) 10. The signal frequency is 50 kHz.

Fig. 23. The measurement results (a)  $A_{out}$ , (b)  $A_{out}$ ,  $B_{out}$  and (c)  $Z_{out}$  of the proposed chip operated with optical incremental sensors. The frequency of optical incremental sensors is 1 kHz.

**Table 3**

Comparisons to previous jobs.

	[4]	[6]	This work
Technology		1.2 $\mu\text{m}$ CMOS 2P2M	0.5 $\mu\text{m}$ CMOS 2P2M
Interpolation methodology	PLL-based	ADC-based	Comparator-based
Sampling frequency	Do not need (VCO is applied)	30 MHz	Do not need
Interpolation factor	70	5, 10, 25, 50	5, 10, 40 (optional)
Output format	Sine signals	Counter code	Pulse stream
Calibration method	None	None	Provided
Chip area	N.A.	13 mm <sup>2</sup>	3 mm <sup>2</sup>
Differential nonlinearity	N.A.	<0.3 counts	<0.5 counts
Integral nonlinearity	N.A.	<0.5 counts	<0.8 counts

less than 1 count. That means that the non-linearity error is all less than  $9^\circ$  under the interpolation number of 10. The proposed chip can attain a characteristic of good linearity.

Finally, measurement results of the proposed chip operated with optical incremental sensors are performed. The frequency of optical incremental sensors is 1 kHz. The interpolation factor is 10. In Fig. 23, the outputs of  $A_{out}$ ,  $B_{out}$ , and  $Z_{out}$  are also successfully obtained. The characteristics of the proposed CMOS phase to digital transducer for optical incremental sensors are summarized in Table 2. The characteristics of the proposed chip are compared with previous jobs and organized in Table 3.

## 5. Conclusion

A CMOS phase to digital transducer for optical incremental sensors is newly proposed. This chip adopts a proposed phase-shift method, which can easily generate phase shifts of signals by using a resistor chain. Owing to the fact that the outputs of the proposed chip are directly digitized, it does not need a ROM component and a faster counter as used in the structures of ADC-based and PLL-based interpolations. The output signals could be also easily sent over a wide range of transmission media, such as PSN, radio, optical, IR, ultrasonic, etc. All the functions and performance of the proposed CMOS phase to digital transducer for optical incremental sensors are successfully tested and proven through measurements. In the future, the developed techniques will be adaptively designed into optical devices, such as optical encoders.

## Acknowledgements

The authors acknowledge Center for Measurement Standards of Industrial Technology Research Institute for their support in optical incremental sensors and also acknowledge Ms. Alice Kao, Mr. Yu-Yuan Chen of Center for Measurement Standards for their technical support in measurement testing.

## References

- [1] K. Araki, T. Tanahashi, S. Kondo, Phase-lock-loop speed control using a micro-computer, in: Proceedings of 18 Annual Symposium Incremental Motion Control System and Devices, 1989, pp. 29–38.
- [2] J.N. Lygouras, K.A. Lalakos, P.G. Ysalides, High-performance position detection and velocity adaptive measurement for closed-loop position control, IEEE Transactions on Instrumentation and Measurement 47 (August (4)) (1998) 978–985.
- [3] C.F. Christiansen, R. Battaiotto, D. Fernandez, E. Tacconi, Digital measurement of angular velocity for speed control, IEEE Transactions on Industrial Electronics 36 (February (1)) (1989) 79–83.
- [4] T. Mura, L. Wang, A high-resolution interpolator for incremental encoders based on the quadrature PLL method, IEEE Transactions on Industrial Electronics 47 (February (1)) (2000) 84–90.
- [5] D.A. Garrett, Muirhead Vactric Components Ltd, Interpolation method and shaft angle encoder, U.S.A. Patent 5,041,829 (1991).
- [6] M. Krauß, U. Leuschner, H.G. Schniek, A. Hilbert, A 5V CMOS chip for interpolation of sine/cosine signals, in: Proceedings of IEEE ESSCIRC, 1997, pp. 336–339.
- [7] E. Schwefel, J. Heidenhain, GmbH. Traunreut, Germany, Interpolation apparatus for digital electronic position measuring instrument, U.S.A. Patent 4,225,931 (1980).
- [8] E. Schwefel, J. Heidenhain, GmbH. Traunreut, Germany, Method of interval interpolation, U.S.A. Patent 4,462,083 (1984).
- [9] W.F.N. Stephens, M.E. Pleydell, Renishaw plc, Gloucestershire, United Kingdom, Interpolation apparatus, U.S.A. Patent 4,949,289 (1990).
- [10] H. Rieder, M. Schwaiger, RSF-Elektronik Gesellschaft m.b.H. Tarsdorf, Austria, Method of electronically correcting position errors in an incremental measuring system and measuring system for carrying out the method, U.S.A. Patent 5,021,650 (1991).
- [11] C.T. Chiang, K.C. Hsieh, Y.C. Huang, A CMOS phase to digital converter for optical encoders, in: Proceedings of IEEE International Instrumentation and Measurement Technology Conference, I<sup>2</sup>MTC'11, May 2011, pp. 1368–1371.
- [12] J.M. Chou, Y.T. Hsieh, J.T. Wu, A 125 MHz 8b digital-to-phase converter, in: Proceedings of IEEE International Solid-State Circuits Conference, February 2003, pp. 436–437.
- [13] P.K. Hanumolu, V. Kratyuk, G.Y. Wei, U.K. Moon, A sub-picosecond resolution 0.5–1.5 GHz digital-to-phase converter, IEEE Journal of Solid-State Circuits 43 (February (2)) (2008) 414–424.
- [14] <http://www.itri.org.tw/chi/tech-transfer/04.asp?RootNodeId=040&NodeId=041&id=1066>.

## Biographies

**Cheng-Ta Chiang** (S'00-M'05) was born in Taiwan, R.O.C., in 1977. He received the B.S. degree in electronics engineering from Chung Yuan Christian University, Jhongli, Taiwan, in 1999, the M.S. degree in biomedical engineering from the National Cheng Kung University, Tainan, Taiwan, in 2001, and the Ph.D. degree in electronics engineering from the National Chiao Tung University, Hsinchu, Taiwan, in 2006.

He was a visiting scholar with the Department of Electrical and Computer Engineering, The Johns Hopkins University, Baltimore, MD, from October 1, 2004 until November 30, 2005. He was included in *Marquis Who's Who in Science and Engineering 2006–2007* and *Marquis Who's Who in the World 2008*. Since 2007, he was a review committee member of the National Chip Implementation Center, Hsinchu. From 2006 to 2010, he was a member of technical staff at Industrial Technology Research Institute, Hsinchu, and was responsible for Nyquist & Oversampled A/D converters, and MEMS circuits. Since 2010, he was with National Chia Yi University, Chiayi, Taiwan, and serviced as an assistant professor in the Department of Electrical Engineering. His main research interests include analog integrated circuits, biomedical electronics, image sensor circuits and systems, sensor signal conditioning and transducers, Nyquist A/D converters, and high-resolution delta-sigma modulator.

Dr. Chiang is a conference reviewer for IEEE conferences of I<sup>2</sup>MTC 2008, ISIEA 2009–2011, PECON 2010, IAPEC 2011, ICEDSA 2011, ICBEIA 2011, PEOCO 2011, CSNT 2011, and a journal reviewer for the IEEE Transactions on Instrumentation and Measurement, IEEE Industrial Electronics, IEEE Sensors Journal, Microelectronics Journal, EURASIP Journal on Advanced in Signal Processing, and an editorial advisory board member for the Sensors & Transducers Journal.

**Kaun-Chun Hsieh** was born in Taiwan, R.O.C., in 1976. He received the B.S. degree in electrical engineering from National Taiwan University and the M.S. degree in electronics engineering from National Chiao Tung University, Taiwan, R.O.C., in 1998 and 2001, respectively. He currently services in Global Unichip Corporation, Hsinchu, Taiwan, R.O.C.

His main research interests have been in analog integrated circuits, and IP services.

**Yu-Chung Huang** received the M.S. degree in electrical engineering and Ph.D. degree in process engineering from the Technology University of Berlin, Berlin, Germany, in 1982 and 1985, respectively.

Since 1985, he has been a Professor in the Department of Electronics, National Chiao Tung University, Hsinchu, Taiwan, R.O.C. His research interests are sensors and measuring technologies.

Prof. Huang is a member of the Committee of the Chinese Metrology Society and a member of the Micromechanical Science Institute, R.O.C.